Check for updates

THE AMERICAN SOCIETY OF MECHANICAL ENGINEERS
Three Park Avenue, New York, N.Y. 10016-5990

99-GT-169

The Society shall not be responsible for statements or opinions advanced in papers or discussion at meetings of the Society or of its Divisions or Sections, or printed in its publications. Discussion is printed only if the paper is published in an ASME Journal. Authorization to photocopy for internal or personal use is granted to libraries and other users registered with the Copyright Clearance Center (CCC) provided $3/article is paid to CCC, 222 Rosewood Dr., Danvers, MA 01923. Requests for special permission or bulk reproduction should be addressed to the ASME Technical Publishing Department.

Copyright © 1999 by ASME All Rights Reserved Printed in U.S.A.

HEAT TRANSFER AND FLOW ON THE FIRST STAGE BLADE TIP OF A POWER GENERATION GAS TURBINE PART 1: EXPERIMENTAL RESULTS

Ronald S. Bunker and **Jeremy C. Bailey**
General Electric Corp. R&D Center
Schenectady, NY, USA

Ali A. Ameri
AYT Corporation, Brook Park, OH, USA

ABSTRACT

A combined experimental and computational study has been performed to investigate the detailed distribution of convective heat transfer coefficients on the first stage blade tip surface for a geometry typical of large power generation turbines (>100MW). This paper is concerned with the design and execution of the experimental portion of the study, which represents the first reported investigation to obtain nearly full surface information on heat transfer coefficients within an environment which develops an appropriate pressure distribution about an airfoil blade tip and shroud model. A stationary blade cascade experiment bas been run consisting of three airfoils, the center airfoil having a variable tip gap clearance. The airfoil models the aerodynamic tip section of a high pressure turbine blade with inlet Mach number of 0.30, exit Mach number of 0.75, pressure ratio of 1.45, exit Reynolds number based on axial chord of $2.57*10^6$, and total turning of about 110 degrees. A hue detection based liquid crystal method is used to obtain the detailed heat transfer coefficient distribution on the blade tip surface for flat, smooth tip surfaces with both sharp and rounded edges. The cascade inlet turbulence intensity level took on values of either 5% or 9%. The cascade also models the casing recess in the shroud surface ahead of the blade. Experimental results are shown for the pressure distribution measurements on the airfoil near the tip gap, on the blade tip surface, and on the opposite shroud surface. Tip surface heat transfer coefficient distributions are shown for sharp-edge and rounded-edge tip geometries at each of the inlet turbulence intensity levels.

NOMENCLATURE

C	Tip gap clearance (mm)
h	Convective heat transfer coefficient (W/m2/K)
k	Thermal conductivity (W/m/K)
LE	Airfoil leading edge designation
Nu	Nusselt number, hC/k_{air}
P/S	Pressure side of airfoil (concave side)
Q_{wall}	Tip surface applied heat flux (W)
Re	Cascade Reynolds number based on airfoil axial chord length and exit conditions
S/S	Suction side of airfoil (convex side)
TE	Airfoil trailing edge designation
$T_{air\ inlet}$	Cascade inlet total air temperature (C)
$T_{surface}$	Mylar surface temperature (C)
Tu	Approach freestream turbulence intensity

INTRODUCTION

The design of high efficiency, highly cooled gas turbines is achieved through the orchestrated combination of aerodynamics, heat transfer, mechanical strength and durability, and material capabilities into a balanced operating unit. While decades of research have been dedicated to the study and development of efficient aerodynamics and cooling techniques for turbine airfoils, there remain regions which retain a somewhat more uncertain design aspect requiring more frequent inspection and repair. One such region particular to high-pressure turbines is the blade tip area. Blade tips are comprised of extended surfaces at the furthest radial position of the blade, which are exposed to hot gases on all sides, typically difficult to cool, and subjected to the potential for wear or even hard rubs against the shroud. It has long been recognized that the effectiveness of the blade tip design and subsequent tip leakage flows is a major contributor to the aerodynamic efficiency of turbines, or the lack thereof. The derivative of turbine efficiency with blade tip clearance can be significant, signaling a strong desire on the part of the designers to improve efficiency by decreasing tip-to-shroud operating

Presented at the International Gas Turbine & Aeroengine Congress & Exhibition
Indianapolis, Indiana — June 7-June 10, 1999
This paper has been accepted for publication in the Transactions of the ASME
Discussion of it will be accepted at ASME Headquarters until September 30, 1999

Downloaded from http://asmedigitalcollection.asme.org/GT/proceedings-pdf/GT1999/78606/V003T01A049/2412453/v003t01a049-99-gt-169.pdf by guest on 21 August 2022

clearances, or by implementing more effective tip leakage sealing mechanisms. There are several blade tip designs in current use within the industry which emphasize various aspects of the total problem. Generally, these designs include flat unshrouded blade tips which use well controlled internal cooling to assure thermal stability, unshrouded tips with various forms of squealer rims to reduce hot gas leakage while providiag protection against shroud rubs, and shrouded blade tips (attached shrouds) which seek to establish high aerodynamic efficiency but with a penalty on blade stresses. High performance versions of these blade tip designs usually also utilize some amount of film cooling to reduce regional heat loads.

No matter the design choice selected for any particular turbine blade tip, a detailed knowledge of the flow field and tip heat transfer is required to achieve the proper balance of elements for efficiency with durability. The flow in and around turbine blade tips has been under investigation much longer than the heat transfer aspects, spurred by the great impact on efficiency for both turbines and compressors. An early work of Lakshminarayana (1970) developed predictive models for stage efficiency and compared these to existing data for several classes of turbomachinery. A comprehensive study by Booth et al. (1982) and Wadia and Booth (1982) measured overall and local blade tip losses for many configurations of tip geometries, and developed predictive methods based on discharge coefficients. Later work of Moore et al. (1989) examined flat tip region flows from laminar to transonic conditions and compared their predictions with available experimental data. More recently, detailed measurements of velocity and pressure fields have been obtained within an idealized tip gap by Sjolander and Cao (1995). The effects of tip clearance, tip geometry, and multiple stages on turbine stage efficiency have lately been quantified by Kaiser and Bindon (1997) within a rotating turbine rig environment. Many other works, too numerous to list here, have studied the effects of tip clearances in axial turbines with the primary emphasis on total leakage and efficiency loss prediction.

Heat transfer on turbine blade tips has been a subject of consistent research over the past fifteen years more or less. Even earlier research dealing with flow and heat transfer over cavities, such as Seban (1965), relates to certain cases of turbine blade tips. Work directly aimed at blade tip heat transfer began with the study of Mayle and Metzger (1982) in which tip average heat transfer coefficients were measured for nominally flat tip models with various flow Reynolds number and rotational speeds. For the parameter ranges tested, they found that the average tip heat transfer was only a weak function of the rotational speed; ie. the average heat transfer was mainly determined by the pressure driven flow through the tip gap. A subsequent study of Metzger et al. (1989) examined the local details of tip heat transfer coefficients for both flat and grooved, stationary rectangular tip models as a function of geometry and Reynolds number, based upon the previous finding that the overall tip driving pressure potential controls the heat transfer. Chyu et al. (1989) then carried this study one step further by introducing a moving shroud surface over the rectangular cavity. Here again it was determined that the relative motion had a minor influence on the average tip heat transfer, though some local effects were observed. Very limited experimental data have been reported in either stationary or rotating cascade environments. Yang and Diller (1995) modeled a turbine blade tip with recessed cavity in a stationary linear cascade, and deduced a local heat transfer coefficient from a heat flux gage placed within the cavity at midchord. Metzger et al. (1991) measured several local tip heat fluxes, primarily in the blade forward region, on the flat tips within a rotating turbine rig at two differing tip clearances. No definitive conclusions were drawn from either of these rig studies.

Additional heat transfer experimental studies have focused on other aspects of blade tips which are equally important to the design of turbines. Metzger and Rued (1989) and Rued and Metzger (1989) performed fundamental studies showing both the flow field and heat transfer characteristics of the blade pressure side sink flow region as leakage enters the tip gap, and the blade suction side source flow region as leakage exits the tip gap, respectively. The effects of film injection on blade tip local heat transfer and film effectiveness distributions using idealized rectangular models is summarized in Kim et al. (1995). Other aspects of turbines which effect blade tip heat transfer include unsteadiness from upstream wakes and secondary flows, injection of coolant sources from the stationary shroud and casing, surface roughness, radial gas temperature profiles and migration, oxidation, and erosion, all of which can have weak or strong influence, but none of which has been investigated in the open literature on heat transfer.

Numerical investigations are playing an increasing important role in the study and design of turbine blade tips for both flow and heat transfer considerations. An earlier work of Chyu et al. (1987) used a two-dimensional finite difference solver to predict the flow and heat transfer in rectangular grooves modeling blade tips, with and without the effects of rotation. More recently, three-dimensional CFD analyses have been performed by Ameri and Steinthorsson (1995, 1996) and Ameri et al. (1997, 1998) showing the predicted effects of tip clearance, tip geometry, and shroud casing for several blade tip designs. While the details of such CFD analyses are astounding, there is still very little validation data available for comparison.

The present study was undertaken in two parallel paths: Part 1 examines the experimental pressure and heat transfer distributions on a stationary blade tip cascade model, while Part 2 compares this data to CFD predictions performed on the same geometry (Ameri and Bunker, 1999). This is the first such study to compare detailed blade tip heat transfer distributions to CFD predictions in the same geometry. The blade tip cascade chosen for this study represents a modern first stage blade of a land-based power turbine. The blade tip geometry is that of a flat tip with a recessed shroud casing and a nominal tip clearance of approximately 1% of the blade height. Tip surface heat transfer is presented for sharp-edge and radius-edge tips, three clearances, and two freestream approach turbulence levels. Pressure distributions are presented for the blade tip and near-tip surfaces, as well as the shroud surface.

EXPERIMENTAL APPARATUS, TEST MODELS, AND TEST METHODOLOGY

The experimental facility used in the present study is a cold-flow, steady-state blade cascade comprised of three airfoils and two airfoil flow passages. The cascade is stationary. Figure 1 shows the overall layout of the facility and cascade test section. The test rig is fed with compressed air from dedicated in-house compressors. Preceding the blade cascade is a flow preparation vessel of 51-cm internal diameter, which contains a front end splash plate to

Downloaded from http://asmedigitalcollection.asme.org/GT/proceedings-pdf/GT1999/78606/V003T01A049/2412453/v003t01a049-99-gt-169.pdf by guest on 21 August 2022

distribute the flow within the vessel and a short section of duct (25 cm length) of the same cross section as the cascade. The vessel also contains a rupture disk for safety against over-pressure. The cascade inlet dimensions are 18.94 cm width by 10.16 cm height (span). The cascade test section is bolted to and sealed against the blind flange face of the vessel. A turbulence generating grid is placed at this juncture, which is composed of 6.35-mm wide square bars with 12.7-mm openings between bars. Hot film anemometry measurements using a TSI IFA-100 unit show that the freestream turbulence intensity level at the cascade blade leading edge plane is 5% for the mainstream flow direction; the turbulence length scale was not measured. After flowing through the cascade, air exits into an exhaust duct of larger area and then to an exterior building vent.

The cascade proper is constructed of aluminum walls and airfoils, with the exception of the shroud cover plate which is 5.08-cm thick acrylic. The flow channel ahead of the blades contains a splitter plate which extends from the turbulence grid to within 12.7 mm of the leading edge of the center airfoil, a distance of about 35.5 cm. The splitter plate divides the channel into equal halves for the purpose of guaranteeing equal flow to each blade cascade passage. Without this device, a substantially greater percentage of the total flow would proceed through the shorter flow passage due to less resistance in that overall path. Pressure traverses made in each of the two channels ahead of the blades verified the 50/50 flow split. These measurements also showed that typical turbulent flow profiles are present downstream of the turbulence grid. The splitter plate is 9.53 mm wide and extends over the entire span. The upstream end of the plate is rounded to minimize flow disturbance, and the downstream end is tapered to a thickness of 3.18 mm and rounded. It is realized that this splitter plate will present some disturbance to the flow field at the very leading edge of the blade, as well as the leading edge of the blade tip gap. The CFD analyses of Part 2 of this study are used to show the effect of this splitter plate on tip flow and heat transfer, thereby providing the necessary aid to interpretation of the present data. Also placed upstream of the blades are optional turbulence bars for use when a higher turbulence intensity is desired. When in use there are four 1.27-cm diameter round bars placed spanwise in each channel at a distance of 10.2 cm ahead of the blade leading edge plane. In this configuration, hot film measurements show a turbulence intensity of 9% at the blade leading edge plane.

Cascade instrumentation which is common to all of the present tests includes an inlet air thermocouple placed midway between the inlet flange and blades, a total pressure wedge probe at the blade leading edge plane midway between two blades, and blade inlet and exit endwall static pressure taps along each passage centerline in the wall opposite the shroud. The total flow for the cascade is measured by an ASME-standard orifice station placed in the air supply pipe lines ahead of the test rig. The nominal operating conditions for this cascade are an inlet total pressure of 160 kPa, an exit static pressure of 110.3 kPa, giving an overall blade pressure ratio of 1.45 when no tip gap is present ($C = 0$). While the inlet flow and total pressure to each of the two cascade passages is equal, the exit conditions are not quite periodic. This is due to the differing exit lengths and the interactions with boundaries. When $C = 0$, the upper passage (concave side of the center airfoil) has a pressure ratio of 1.47, while the lower passage is 1.43, based upon exit static pressures measured in the endwall at the blade root. For the average tip clearance tested, $C = 2.03$ mm, the passages each have lower individual pressure ratios of 1.41 and 1.33, for upper and lower passages respectively. This change is due to the leakage of air over the tip from upper to lower passage, and the existence of a flow gap over the airfoil trailing edge base. Experimentally this is not a problem, as long as the blade tip pressures are known and are representative of a typical pressure distribution driving the tip leakage. The nominal total flow rate for the cascade section is 3.4 kg/sec, and the typical inlet air total temperature is 22 C. The inlet air velocity approaching the blades is 101 m/s and the corresponding Mach number is 0.30.

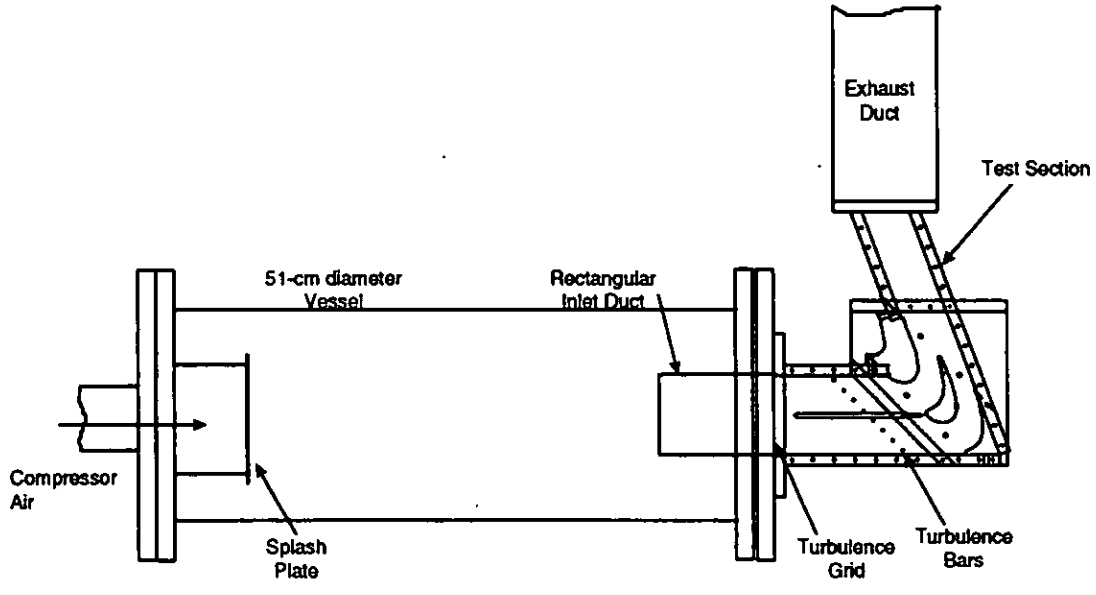

Figure 1. Blade Tip Cascade Facility

Downloaded from http://asmedigitalcollection.asme.org/GT/proceedings-pdf/GT1999/78606/V003T01A049/2412453/v003t01a049-99-gt-169.pdf by guest on 21 August 2022

The definition of the airfoil placement is depicted in Figure 2. The airfoils are constant cross section for the entire span (linear cascade) and represent the tip section of an aerodynamic blade design. The inlet flow angle to the test airfoil is 44.9 degrees and the exit angle is 65.75 degrees, giving a total turning of 110.65 degrees. The blade leading edge pitch is 13.37 cm. The axial chord length of the blade is 12.45 cm. The throat diameter at the point of minimum distance between two blades is 5.19 cm, which with a span of 10.16 cm gives a throat aspect ratio of about 2. The center airfoil is the test airfoil and as such is designed to allow variable insertion depths into the cascade to change the tip gap clearance beneath the acrylic shroud cover. Figure 2 also shows the shroud surface relative to the airfoils. The shroud contains a 2 mm step placed 3.43 cm ahead of the blade leading edge plane, which models a similar feature found in the turbine shroud. Additionally, a boundary layer trip is placed on the shroud wall 1.27 cm ahead of the step to ensure a fresh boundary layer approaches the blade tip and shroud flow region.

The tip clearances used in the present study vary from 1.27 to 2.79 mm and are constant over the entire blade tip. Only the center airfoil contains this tip clearance to allow leakage flow from the pressure side to the suction side of the airfoil. An Aluminum test airfoil having pressure taps around the entire perimeter of the airfoil, was first placed in the center location of the cascade. Surface holes of 0.5 mm diameter were located 3.2 mm down from the blade tip to measure the near-tip airfoil pressure distribution without a tip clearance, and also with a clearance of 2.03 mm. These two pressure distributions are shown together in Figure 3, where the airfoil local surface axial positions have been normalized by the axial chord length. These distributions show the effect of the gap leakage in modifying the pressure field which ultimately drives the local leakage strengths and the resulting heat transfer. With the tip gap present, the Mach distribution is shifted "toward" the aft portion of the airfoil, which is consistent with expected leakage paths and strengths. At the tip section then, the exit Mach number for the test airfoil is 0.75. The corresponding airfoil Reynolds number is $2.57 \cdot 10^6$, based upon axial chord length and exit flow conditions. A separate blade having pressure measurement taps located on the tip surface, as well as a shroud plate with pressure taps opposite the blade tip surface, were used to obtain pressure field surveys within the tip gap. These surfaces and distributions will be shown in a later section of this paper.

For blade tip heat transfer testing, another central blade model was fabricated with specific features. Figure 4 shows the basic construction of this model. The lower half of the blade is made of Aluminum for structural rigidity against the aerodynamic forces present during tests. This lower blade section is affixed to the bottom endwall; shims allow adjustment of the tip clearance. The upper half of the blade model is fabricated mainly of acrylic for good insulation against heat losses. The tip itself is comprised of a 6.35-mm thick tip cap made of G7 (an insulating material), which is fit

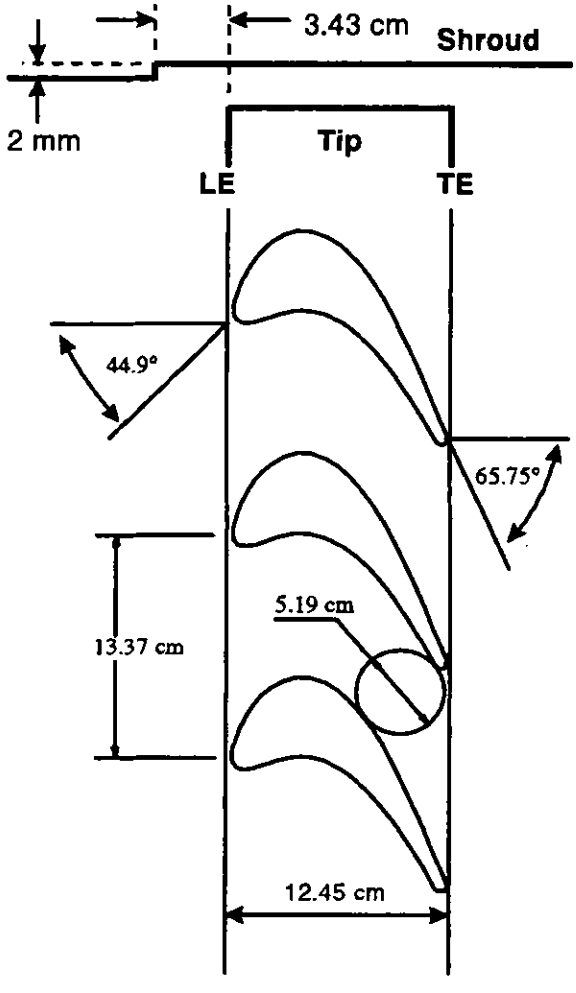

Figure 2. Airfoil and Shroud Definition

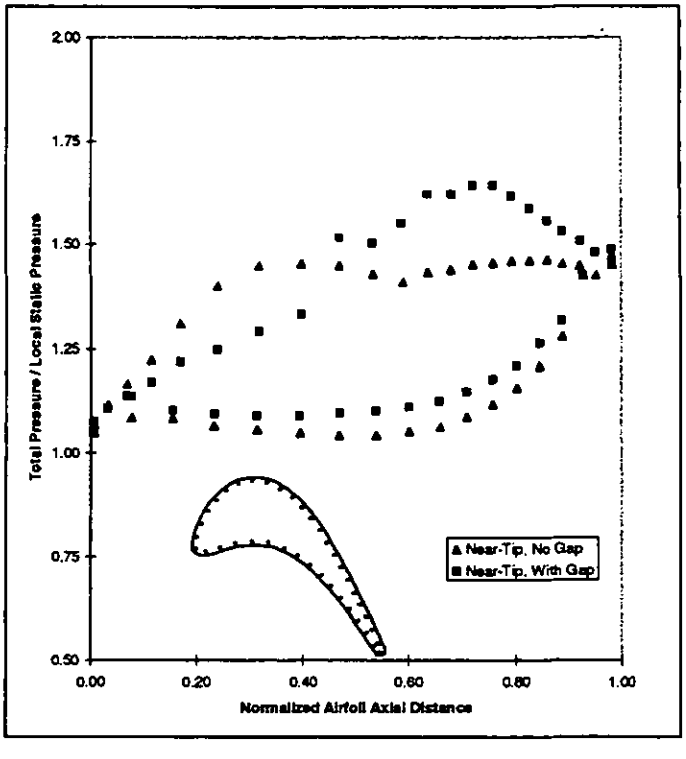

Figure 3. Airfoil Near-Tip Pressure Distributions

Downloaded from http://asmedigitalcollection.asme.org/GT/proceedings-pdf/GT1999/78606/V003T01A049/2412453/v003t01a049-99-gt-169.pdf by guest on 21 August 2022

into a recess within the acrylic and sealed around all edges of the recess shelf. The width of the remaining edge of acrylic outside the G7 is 3.18 mm. The aft-most portion of the narrow trailing edge tip surface which does not contain the recess is about 19 mm in length. Between the G7 cap and the body of the acrylic blade is an air gap of 6.35 mm depth. This air gap serves as insulation, as well as giving access for the placement of monitoring thermocouples on the underside of the G7, which are routed out through a hole in the blade root. Two such tip models were made for this study, one with sharp tip edges (shown in figure), and the other with rounded edges of 2.54 mm radius. The exteat of the tip cap is the same for each of these models.

The top surface of the G7 is covered by an etched thin-foil heater encased in Kapton, which was custom manufactured in the shape of the blade cross section. The heater is then covered by a 0.05 mm thick layer of copper to assist in spreading the heat source from the etched foil circuit to form a uniform heat flux condition. The copper layer is covered with a sheet of liquid crystals. The liquid crystals used in this study are wide hand 40 to 45 C crystals made by Hallcrest (R40C5W). The liquid crystals are located beneath a 0.127 mm thick Mylar encapsulation layer. This Mylar layer is constant in thickness, with a thermal conductivity of 0.145 W/m/K.

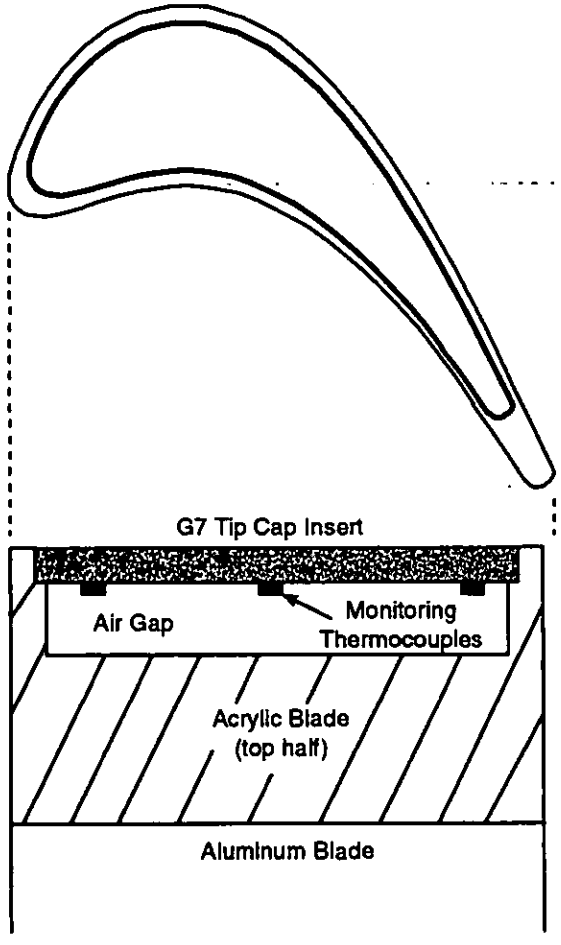

Figure 4. Heat Transfer Blade Tip Construction

The temperature drop across the Mylar layer is accounted for in determining the tip surface temperature seen by the flow. All tests were run by maintaining a steady mainstream flow at the noted Reynolds number, and varying the heater power to allow various regions of the liquid crystals to display color as viewed through the clear shroud wall. The typical heater input power ranged from 40 to 150 W over a total surface area of 46.5 cm^2 for the sharp-edge tip, or 33.7 cm^2 for the radius-edge tip. Note that in all tests performed, only the tip cap portion of the cascade received a surface heat flux, all other surfaces remained unheated. In this respect, the cascade operates differently from an actual turbine in that the cascade blade tip does not attain the same heat flux direction or wall-to-gas temperature ratios as a turbine blade tip, hence additional adjustments must be made to apply such data to turbine conditions. Such adjustments must also be made to account for the reality of work extraction in a rotating turbine. All cascade model surfaces were smooth.

The general hue intensity method as described by Hollingsworth et al. (1989) and Farina and Moffat (1994) was used to deduce temperature from the liquid crystal responses. A separate calibration test stand was utilized for each sheet of liquid crystals as applied to the tip models, to determine the hue-temperature calibration curves. Liquid crystal calibrations followed the illuminant invariant method of Farina et al. (1994). Each blade tip heat transfer contour plot shown in this study is the result of some six or seven images obtained with differing heat fluxes which are combined together. The agreement in data within the overlapping regions of individual images is always found to be excellent.

The primary heat loss present during operation of the cascade amounts to the energy which is not going into the air, but rather is lost via conduction into the blade model and eventual convection into the air of the blade passage flows. This loss was estimated by running the cascade at nominal flow with a zero clearance gap. The tip was pushed up against the shroud with a small amount of perimeter sealing to avoid tip flow leakage and thermal conduction into the shroud. The heater power was adjusted until the liquid crystal layer and the several underside monitoring thermocouples gave the same temperature reading. The heat loss determined in this manner was 4% of the average total heater power. Heat transfer data shown accounts for this loss. Thermal radiation loss is estimated to be less than 1% of the total power for all conditions and is considered negligible.

The definition of the local heat transfer coefficient in this study is

$$h = Q_{wall} / (T_{surface} - T_{air\ inlet})$$

where Q_{wall} is the input heater power per unit area, and $T_{surface}$ is the liquid crystal indicated temperature adjusted for the Mylar layer. In the present results, $T_{air\ inlet}$ is the total cascade inlet air temperature. The experimental uncertainty in local heat transfer coefficient defined in this manner is estimated to be $\pm 8\%$ or better using the methods of Kline and McClintock (1953). The controlling factor in the uncertainty is the driving temperature potential between the total air temperature and the local tip surface temperature of the Mylar. In all cases, a minimum value of 14 C was maintained for this temperature difference.

Downloaded from http://asmedigitalcollection.asme.org/GT/proceedings-pdf/GT1999/78606/V003T01A049/2412453/v003t01a049-99-gt-169.pdf by guest on 21 August 2022

TIP AND SHROUD PRESSURE MEASUREMENTS

In addition to the static pressure measurements obtained on the airfoil pressure and suction side surfaces, pressure measurements were also made on both the shroud surface opposite the blade tip and on the blade tip surface. A separate acrylic shroud cover was fabricated with over 100 holes located above the central blade tip region. All of the pressure holes were 1.59 mm diameter holes machined into the acrylic, with short length 0.51 mm diameter through-holes to the flow path surface. A 48-channel automated Scanivalve system was used to record the pressures for various groups of measurement locations. On this shroud surface, one set of pressure holes was located around the airfoil tip perimeter and 2.54 mm outside the tip edge, while a second set of holes was located 2.54 mm inside the tip edge. Other pressure holes were placed over the interior region above the tip. Figure 5 shows the shroud pressure distribution, in the form of pressure ratios for consistency, over the sharp-edge blade tip model with a clearance of 2.03 mm. The inset figure shows the locations of the pressure holes relative to the tip. The "outer" pressure side (*P/S*) and suction side (*S/S*) data represent the measurements just prior to flow entry into the gap or just after exit from the gap, respectively. Likewise, the "inner" data represent measurements just inside the tip edges. The "mean camber" data are located above the blade mean chord line. As the data show, there is little difference in pressures over the forward 30% of the airfoil, but over the remaining portion there is a large pressure drop associated with the pressure side entry into the gap clearance. Some recovery is observed as the mean camber line is reached, and a bit more as the suction side exit is approached. The final difference in pressure ratios from the pressure side outer to the suction side outer locations is nearly the same as that shown for the near-tip, with gap, airfoil measurements of Figure 3. The same measurements were made for the blade tip model with perimeter radius edge, leading to very similar results.

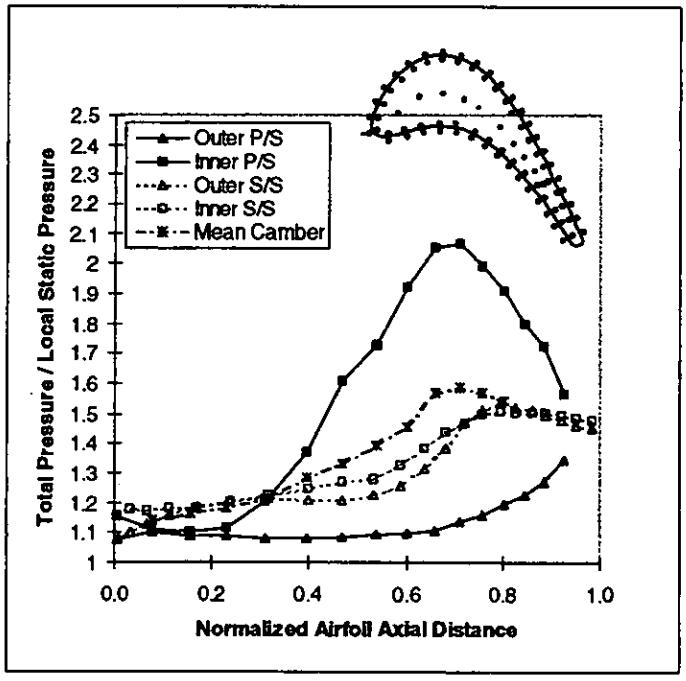

Figure 5. Shroud Surface Pressure Distribution with Sharp-Edge Blade Tip and 2.03 mm Clearance

For the blade tip surface pressure measurements a separate Aluminum tip model was made with similar pressure holes arrayed in the tip surface. In this case, a set of holes was placed around the perimeter and offset 5.08 mm to the interior of the sharp tip edge. Additional pressure holes were located in the interior region to measure the mean camber line pressures. Figure 6 shows the pressure distributions for the sharp-edge tip model for each of three tip gap clearances. The suction side pressures are for the most part essentially the same for each clearance. The pressure side data also show no effect of clearance over the forward 40% of the tip. The aft portion of the tip, however, shows an increasing pressure differential between *P/S* and *S/S* as the clearance is increased, and this change is primarily due to a large decrease in *P/S* gap inlet pressure. This decreasing pressure has an associated higher local flow velocity which will be reflected in the tip heat transfer data shown later. Also of note, is the downturn in *P/S* pressure ratios towards the trailing edge region of the tip. In this region there is less direct *P/S* to *S/S* gap leakage as the passage flow streams come to similar velocities.

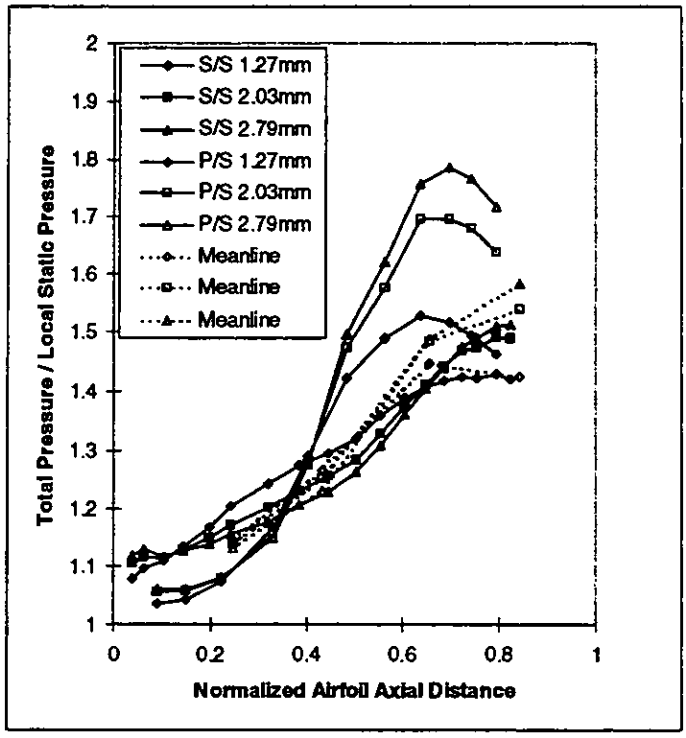

Figure 6. Blade Tip Surface Pressure Distribution with Sharp-Edge Tip and Variable Clearance

The bulk of direct tip gap leakage is then in the 40 to 90% axial chord range, though leakage also occurs from forward locations on the pressure side to midchord locations on the suction side. These tip surface pressure distributions were also measured for a radius edge tip having a 2.54 mm radius around the perimeter of the tip. The effect of this tip edge radius is shown in Figure 7, where the *P/S* entry pressure loss is clearly more dependent upon the clearance height. A distinction in *P/S* measurements is seen beginning as far forward as 30% axial chord location. The smaller

Downloaded from http://asmedigitalcollection.asme.org/GT/proceedings-pdf/GT1999/78606/V003T01A049/2412453/v003t01a049-99-gt-169.pdf by guest on 21 August 2022

clearances of 1.27 and 2.03 mm show higher *P/S* pressure ratios than their sharp edge counterparts, and each of the three *P/S* distributions peak at differing locations. The radius appears to have a definite effect in some redistribution of flow and flow strength into the gap. Little effect is observed on the *S/S* pressures.

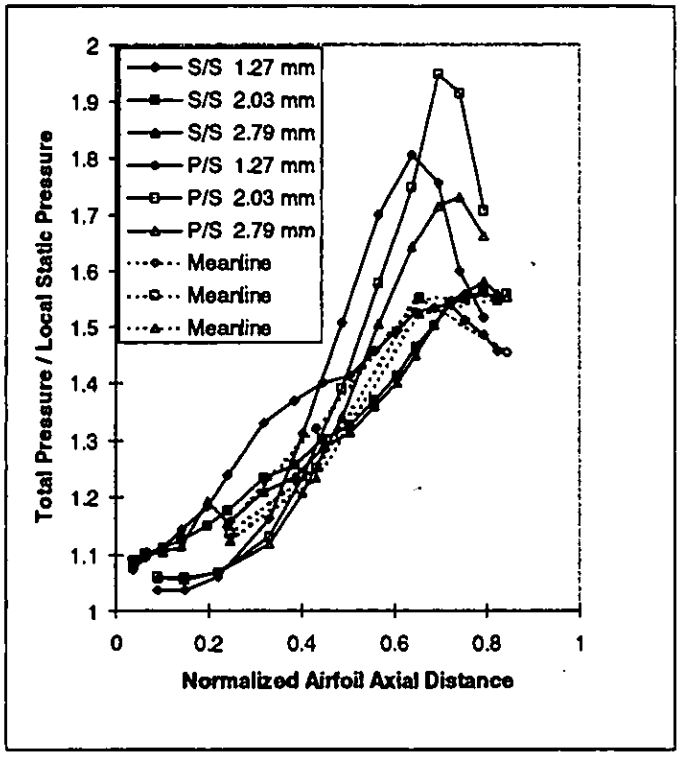

Figure 7. Blade Tip Surface Pressure Distribution with Radius-Edge Tip and Variable Clearance

HEAT TRANSFER RESULTS

Tip surface heat transfer coefficient contour plots are shown for both sharp-edge and radius-edge tip models. In the case of the sharp-edge tip model, the surface heater and liquid crystal layer extend to very nearly the edge of the blade tip. Data for the far edges of the tip surface should be considered less reliable since there does exist some two-dimensional conduction here, as well as slightly less heat flux uniformity. In the case of the radius-edge tip model, the surface heater and liquid crystal layer cover less area, being offset to the interior to allow for the edge radius; ie. the heater does not extend into the radius. Hence, the extent of data is less for the radius tip model. Approximate blade profile overlays are provided in the figures to help in judging these differences. Additionally, regions of very high heat transfer coefficieats tend to be more difficult to acquire with a single liquid crystal type, since these regions may require heat fluxes resulting in temperatures that exceed material capabilities. Such limitation is most notable in the absence of full data in the trailing edge regions of some tests.

Figure 8 shows the tip heat transfer coefficient contour map for the sharp-edge tip model with a nominal tip clearance gap of 2.03 mm and an approach freestream turbulence intensity of 5%. The distribution of heat transfer coefficient seen here is typical in overall aspects for every case tested in this study; number labels are provided for the following description. Most apparent in this distribution is the development of a low heat transfer region within the thickest portion of the tip, what one might refer to as the "sweet spot" (1). This region emanates from the airfoil pressure side location associated with the diffusion zone in Figure 3, at about 20 to 30% axial chord location (2). The low heat transfer region extends into the central area of the tip and appears to extend aft and towards the suction side. This sweet spot is the area of lowest convective velocity on the tip as seen in the tip pressures of Figure 6. At about 30 to 35% axial chord the *P/S* and *S/S* tip pressures are nearly equal. The tip flow forward of this location proceeds across the leading edge region from *P/S* to *S/S* essentially at right angles to the tip meanline, producing high heat transfer coefficients there (3). The tip flow aft of the *P/S* diffusion location encounters a large entry region pressure loss, clearly seen in Figure 6, as it enters the *P/S* of the gap. This entry loss is seen in the bending of the heat transfer coefficient contours near the *P/S* midchord, creating high local heat transfer gradients (4). The sweet spot conforms around this heavy entry loss area, channeling flow down the mean camber line to the suction side (5). It is postulated that there is a separation vortex in this *P/S* entry region of the midchord, with similar roll up and bending toward the airfoil trailing edge as seen in Sjolander and Cao (1995). The portion of the tip suction side from the leading edge around the sweet spot exhibits increasing heat transfer from the center of the tip outwards with isopleths of the same shape as the suction side profile. The high thermal gradients here are a result of the accelerating leakage flow exiting the tip gap (6). In the trailing edge region of about 50% axial chord and aft, leakage flow proceeds mostly straight across from *P/S* to *S/S*, except as modified by the entry region separation. Suction side heat transfer coefficients in the trailing edge are observed to be increasing with regularity as one proceeds aft, with the isopleths (lines of constant heat transfer coefficient) aligned at right angles to the suction side exit (7).

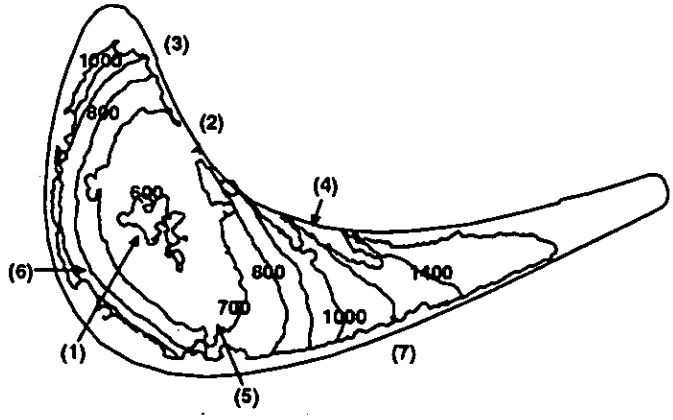

Figure 8. Sharp-edge blade tip heat transfer coefficients for 2.03 mm clearance and *Tu*=5%. (W/m2/K)

Altering the approach freestream turbulence intensity level from 5 to 9% by means of the circular rods installed upstream of the airfoils results in the tip heat transfer coefficient distribution shown in Figure 9. The pattern of heat transfer is seen to be the same as

Downloaded from http://asmedigitalcollection.asme.org/GT/proceedings-pdf/GT1999/78606/V003T01A049/2412453/v003t01a049-99-gt-169.pdf by guest on 21 August 2022

that of Figure 8. The heat transfer magnitude in the central sweet spot is about 10% greater in this case. Heat transfer in the leading edge region is altered but little over the *Tu*=5% result, however that in the trailing edge region aft of the sweet spot is as much as 20% higher. The increase in approach *Tu* level is not expected to change the magnitude of tip leakage flow, but only to adjust the tip local heat transfer. It appears that the increased *Tu* level has had little effect on tip heat transfer over the forward 50% of the tip, but has a not insubstantial effect on the high leakage portion of the blade tip.

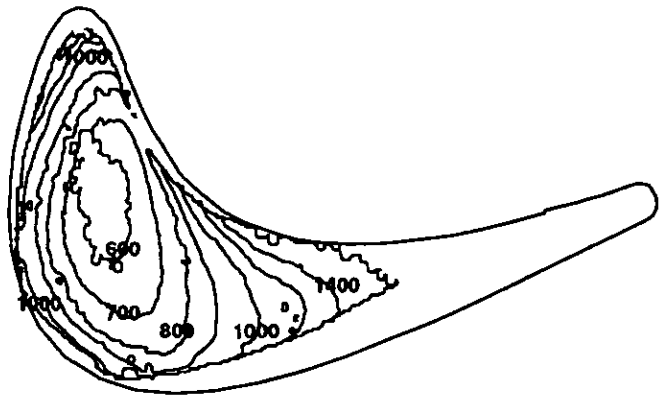

Figure 9. Sharp-edge blade tip heat transfer coefficients for 2.03 mm clearance and *Tu*=9%. (W/m2/K)

Using this tip heat transfer result as more representative of a turbine blade, ie. higher *Tu*, a portion of the tip heat transfer was compared to existing literature results. Figure 10 shows the heat transfer coefficients along a single trajectory starting at about 40% axial chord on the *P/S* and ending at about 60% axial chord on the *S/S*. This trajectory follows a line from *P/S* to *S/S* within the midchord region which experiences an entry separation followed by reattachment and flow to the exit. Recalling that this is a sharp-edge tip, the result is compared to two cases from the work of Boelter et al. (1948) as presented in Kays and Crawford (1980), (1) the case of heat transfer in the entry of a sudden contraction, and (2) the case of heat transfer with fully developed flow prior to a heated section. For the blade tip, the hydraulic diameter is taken to be clearance *C*. Using the overall driving pressure for this trajectory from Figure 3, the resulting Re_C is 38,750. The correlation for fully developed turbulent channel flow heat transfer, $Nu_o = 0.023\ Re^{0.8}\ Pr^{0.4}$, yields a developed heat transfer coefficient for this location of 1050 W/m2/K. This heat transfer level is within 5% of the measured value on the blade tip where the isopleth begins to level out at a minimum (refer to the H=1000 isopleth in Figure 9). The present example of data has insufficient resolution in the entry region to define the heat transfer within $x/C < 1$, but the data does lie between the cases (1) & (2) of Boelter et al. The present geometry can be expected to lie between these extremes since the entry flow is not strictly normal to the tip edge, but swept into the gap with a streamwise component of flow. Also, the tip model has a sudden contraction on only one side. The exiting region of the tip flow shows an increase over fully developed heat transfer due to the modification of acceleration and turning. This example shows that certain regions of the present blade tip model do conform to the simple pressure driven heat transfer behavior demonstrated in previous research such as that of Metzger et al. (1989). It is interesting to note that Metzger et al. (1989) also found flat tip heat transfer in their rectangular model geometry to be lower than that of the sudden contraction entry of Boelter et al. (case 1), in fact their result was nearly the same as the present study.

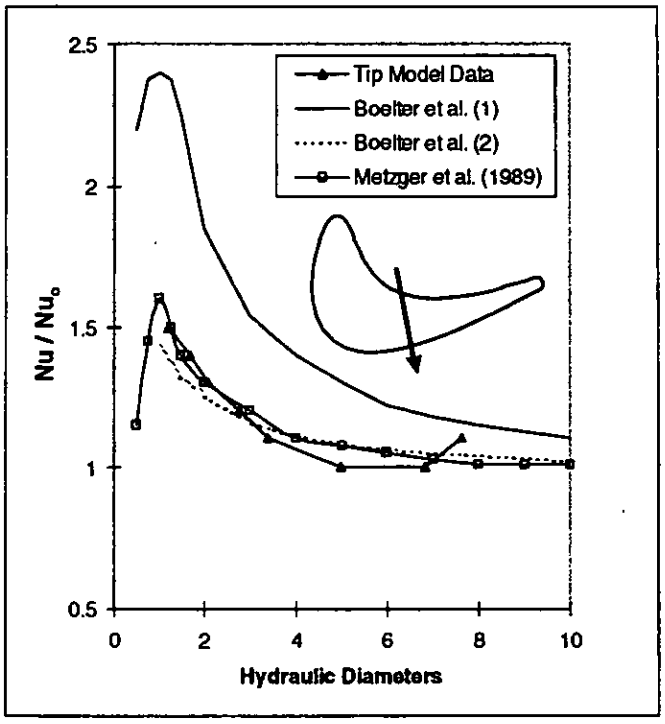

Figure 10. Comparison of selected tip data with pipe entry region data of Boelter et al. (1948) and tip model data of Metzger et al. (1989).

The second blade tip geometry tested in this study was that with a simple radius tip edge. A constant radius of 2.54 mm was formed around the entire perimeter of the blade tip. The purpose of the radius is to provide some easement to the sharp-edged entry which the *P/S* leakage flow sees, as well as providing a better representation of expected blade tip features in service. Figure 11 shows the radius edge tip heat transfer coefficient distribution with a clearance gap of 2.03 mm and approach *Tu* of 5%. Compared to the sharp edge case of Figure 8, the tip heat transfer is here is about 10% higher in most regions. This increase might be attributed to the reduced resistance to tip leakage caused by the radius edge, thereby allowing more total leakage flow and subsequently higher heat transfer, though the effects of tip pressure distributions as shown in Figure 7 can be somewhat subtle in redistributing leakage flows. Figure 12 shows heat transfer for the same tip with an approach *Tu* of 9%. Here too, the tip heat transfer has been increased by 10 to 15% over that of the sharp edge shown in Figure 9. The relation between radius edge tip heat transfer at *Tu* of 5% and 9% is the same as that previously described for the sharp edge cases, a moderate increase in the sweet spot and a somewhat higher increase in the midchord and aft regions.

Downloaded from http://asmedigitalcollection.asme.org/GT/proceedings-pdf/GT1999/78606/V003T01A049/2412453/v003t01a049-99-gt-169.pdf by guest on 21 August 2022

Finally, Figures 13 and 14 show tip heat transfer coefficient distributions for the radius edge model with altered tip gap clearances of 1.27 mm and 2.79 mm, respectively, both at *Tu* of 9%. These changes to the clearance amount to ± 38% of the nominal gap height of 2.03 mm, or on the basis that nominal clearance is 1% of total blade height in a typical turbine then this change is ± 0.38% of blade height. Tightening the tip clearance serves to decrease heat transfer by about 10% due to a reduced tip leakage flow. The sweet spot of Figure 13 appears to be broader, especially in it's extent into the midchord region on the suction side of meanline. Increasing the tip clearance serves to increase tip heat transfer by about the same amount of 10% due to more tip leakage flow.

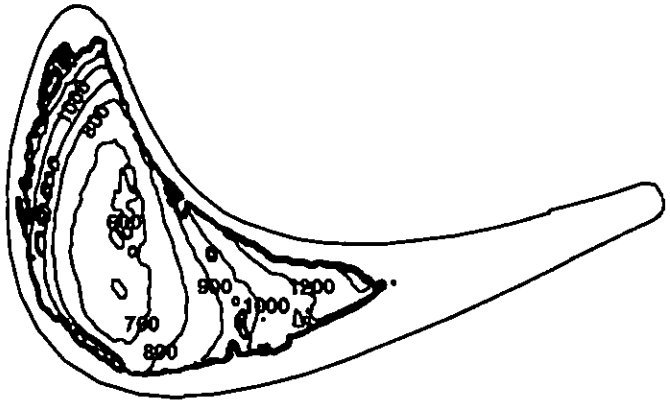

Figure 11. Radius-edge blade tip heat transfer coefficients for 2.03 mm clearance and *Tu*=5%. (W/m2/K)

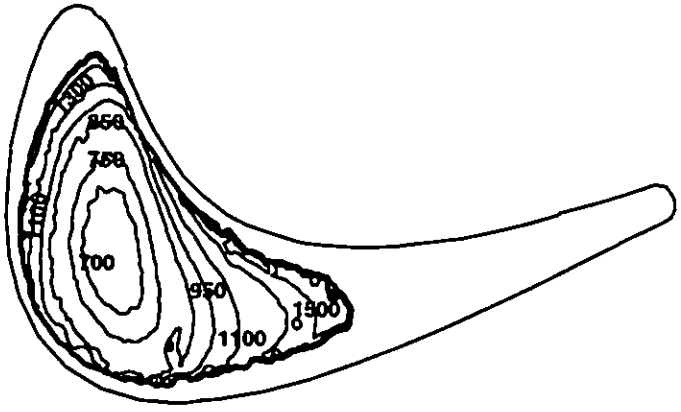

Figure 12. Radius-edge blade tip heat transfer coefficients for 2.03 mm clearance and *Tu*=9%. (W/m2/K)

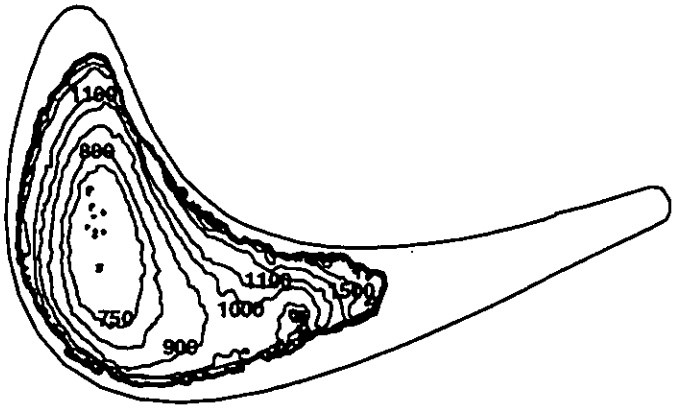

Figure 13. Radius-edge blade tip heat transfer coefficients for 1.27 mm clearance and *Tu*=9%. (W/m2/K)

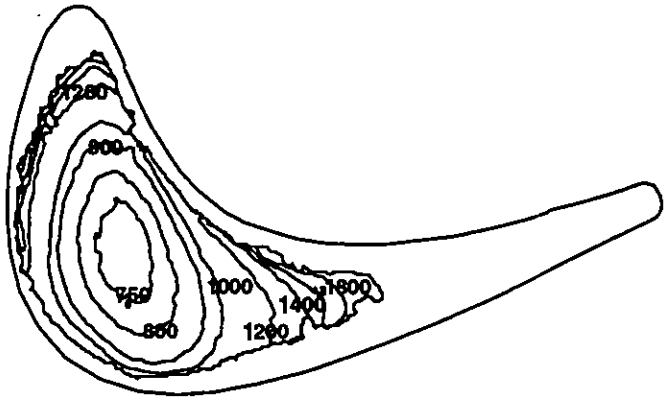

Figure 14. Radius-edge blade tip heat transfer coefficients for 2.79 mm clearance and *Tu*=9%. (W/m2/K)

CONCLUSIONS

The present study has utilized a linear airfoil cascade for the express purpose of examining the detailed heat transfer coefficient distributions on the tip surface of a blade model. This is the first reported study of this type that obtains nearly full surface information on heat transfer coefficients within an environment which develops an appropriate pressure distribution about an airfoil blade tip and shroud model. The blade tip model employed is representative of a typical power turbine, having an airfoil Reynolds number of $2.57 \cdot 10^6$ and an overall pressure ratio of 1.45. The major findings of this study may be summarized as follows:

- In this stationary cascade model, the pressures measured on the airfoil in the near-tip region form a good basis for determining the overall pressure driven tip leakage flows. Details of the pressure field on the tip surface are required to fully explain the heat transfer results, even for the simple case of a flat blade tip.
- Shroud pressure measurements agree well with the tip surface pressures in this setting, showing much the same local characteristics.

Downloaded from http://asmedigitalcollection.asme.org/GT/proceedings-pdf/GT1999/78606/V003T01A049/2412453/v003t01a049-99-gt-169.pdf by guest on 21 August 2022

- Tip entry flow for the sharp edge case exhibits differing character at various positions along the pressure side, with a marked high entry loss region in the midchord-to-aft region. Addition of a small tip edge radius serves to redistribute this entry effect and lead to greater leakage at nominal clearance (as deduced from higher tip heat transfer levels).
- The present tip geometry and flow field demonstrate a characteristic central sweet spot of low heat transfer which extends into the midchord region and toward the suction side. A pressure side entry separation vortex aft of the sweet spot creates a significant enhancement to heat transfer aft of the sweet spot. Large heat transfer coefficient gradients are observed at outlying suction side peripheral areas in the forward half of the airfoil tip.
- An increase in the approach freestream turbulence intensity level from 5 to 9% raises the overall tip heat transfer by about 10%, moreso in the aft portion of the tip (~20%) and less in the forward areas (~0%).
- The addition of a small edge radius to the tip perimeter causes the tip heat transfer to increase by about 10% in most areas, presumably due to higher allowed tip leakage flow.
- Decreasing the tip clearance C by 38% of the nominal value results in a decrease of some 10% in heat transfer, while an equivalent increase in tip clearance results in a 10% increase in heat transfer.
- Certain regions of the present tip model appear to conform to a simple pressure driven heat transfer behavior similar to that of entry flow into a sudden contraction, but with significant local modifications due to the 3D nature of the flow.

For all of the cases studied here, the blade tip heat transfer coefficient distributions show similar features. The variety of regional effects though points to a very three-dimensional problem even for this stationary case. The data obtained under these simplified conditions is used for comparison to 3D CFD predictions of the flow and heat transfer in the blade tip region, which is the subject of Part 2 of this study

ACKNOWLEDGEMENT

This study was prepared with the support of the U.S. Department of Energy, under Cooperative Agreement No. DE-FC21-95MC31176. However, any opinions, findings, conclusions, or recommendations expressed herein are those of the author and do not necessarily reflect the views of the DOE.

REFERENCES

Ameri, A.A. and Bunker, R.S., 1999, "Heat Transfer and Flow on the First Stage Blade Tip of a Power Generation Gas Turbine Part 2: Simulation Results", to be presented at the 1999 IGTI Turbo Expo, Indianapolis, USA.

Ameri, A.A. and Steinthorsson, E., 1995, "Prediction of Unshrouded Rotor Blade Tip Heat Transfer", 95-GT-142, Int. Gas Turbine Conference, Houston, USA.

Ameri, A.A. and Steinthorsson, E., 1996, "Analysis of Gas Turbine Rotor Blade Tip and Shroud Heat Transfer", 96-GT-189, Int. Gas Turbine Conference, Birmingham, UK.

Ameri, A.A., Steinthorsson, E., and Rigby, D.L., 1997, "Effect of Squealer Tip on Rotor Heat Transfer and Efficiency", 97-GT-128, Int. Gas Turbine Conference, Orlando, USA.

Ameri, A.A., Steinthorsson, E., and Rigby, D.L., 1998, "Effects of Tip Clearance and Casing Recess on Heat Transfer and Stage Efficiency in Axial Turbines", 98-GT-369, Int. Gas Turbine Conference, Stockholm, Sweden.

Boelter, L.M.K., Young, G., and Iversen, H.W., 1948, "An Investigation of Aircraft Heaters XXVII - Distribution of Heat Transfer Rate in the Entrance Region of a Tube", NACA TN 1451.

Booth, T.C., Dodge, P.R., and Hepworth, H.K., 1982, "Rotor-Tip Leakage: Part I - Basic Methodology", *J. of Engineering for Power*, Vol. 104, pp. 154-161.

Chyu, M.K., Metzger, D.E., and Hwan, C.L., 1987, "Heat Transfer in Shrouded Rectangular Cavities", *J. of Thermophysics*, Vol. 1, No. 3, pp. 247-252.

Chyu, M.K., Moon, H.K., and Metzger, D.E., 1989, "Heat Transfer in the Tip Region of Grooved Turbine Blades", *J. of Turbomachinery*, Vol. 111, pp. 131-138.

Farina, D.J., Hacker, J.M., Moffat, R.J., and Eaton, J.K., 1994, "Illuminant Invariant Calibration of Thermochromic Liquid Crystals", *Experimental Thermal and Fluid Science*, Vol. 9, pp. 1-9.

Farina, D.J. and Moffat, R.J., 1994, "A System for Making Temperature Measurements Using Thermochromic Liquid Crystals", Report No. HMT-48, Thermosciences Division, Stanford University.

Hollingsworth, D.K., Boehman, A.L., Smith, E.G., and Moffat, R.J., 1989, "Measurement of Temperature and Heat Transfer Coefficient Distributions in a Complex Flow Using Liquid Crystal Thermography and True-Color Image Processing", *ASME Collected Papers in Heat Transfer*, pp. 35-42.

Kaiser, I. And Bindon, J.P., 1997, "The Effect of Tip Clearance on the Development of Loss Behind a Rotor and a Subsequent Nozzle", 97-GT-53, Int. Gas Turbine Conference, Orlando, USA.

Kays, W.M. and Crawford, M.E., 1980, *Convective Heat and Mass Transfer*, Second Edition, McGraw-Hill, pg. 269.

Kim, Y.W., Abdel-Messeh, W., Downs, J.P., Soechting, F.O., Steuber, G.D., and Tanrikut, S., 1995, "A Summary of the Cooled Turbine Blade Tip Heat Transfer and Film Effectiveness Investigations Performed by Dr. D.E. Metzger", *J. of Turbomachinery*, Vol. 117, pp. 1-11.

Kline, S.J. and McClintock, F.A., 1953, "Describing Uncertainties in Single Sample Experiments", Mechanical Engineering, Vol. 75, January, pp. 3-8.

Lakshminarayana, B., 1970, "Methods of Predicting the Tip Clearance Effects in Axial Flow Turbomachinery", *J. of Basic Engineering*, Vol. 92, pp. 467-482.

Mayle, R.E. and Metzger, D.E., 1982, "Heat Transfer at the Tip of an Unshrouded Turbine Blade", *Proc. Seventh Int. Heat Transfer Conf.*, Hemisphere Pub., pp. 87-92.

Metzger, D.E., Bunker, R.S., and Chyu, M.K., 1989, "Cavity Heat Transfer on a Transverse Grooved Wall in a Narrow Flow Channel", *J. of Heat Transfer*, Vol. 111, pp. 73-79.

Metzger, D.E., Dunn, M.G., and Hah, C., 1991, "Turbine Tip and Shroud Heat Transfer", *J. of Turbomachinery*, Vol. 113; pp. 502-507.

Metzger, D.E. and Rued, K., 1989, "The Influence of Turbine Clearance Gap Leakage on Passage Velocity and Heat Transfer Near

Downloaded from http://asmedigitalcollection.asme.org/GT/proceedings-pdf/GT1999/78606/V003T01A049/2412453/v003t01a049-99-gt-169.pdf by guest on 21 August 2022

Blade Tips: Part I - Sink Flow Effects on Blade Pressure Side", *J. of Turbomachinery*, Vol. 111, pp. 284-292.

Moore, J., Moore, J.G., Henry, G.S., and Chaudhry, U., 1989, "Flow and Heat Transfer in Turbine Tip Gaps", *J. of Turbomachinery*, Vol. 111, pp. 301-309.

Rued, K. and Metzger, D.E., 1989, "The Influence of Turbine Clearance Gap Leakage on Passage Velocity and Heat Transfer Near Blade Tips: Part II - Source Flow Effects on Blade Suction Sides", *J. of Turbomachinery*, Vol. 111, pp. 293-300.

Seban, R.A., 1965, "Heat Transfer and Flow in a Shallow Rectangular Cavity with Subsonic Turbulent Air Flow", *Int. Journal of Heat and Mass Transfer*, Vol. 8, pp. 1353-1368.

Sjolander, S.A. and Cao, D., 1995, "Measurements of the Flow in an Idealized Turbine Tip Gap", *J. of Turbomachinery*, Vol. 117, pp. 578-584.

Wadia, A.R. and Booth, T.C., 1982, "Rotor-Tip Leakage: Part II - Design Optimization Through Viscous Analysis and Experiment", *J. of Engineering for Power*, Vol. 104, pp. 162-169.

Wehner, M., Buetikofer, J., Hustad, C-W., and Boelcs, A., 1997, "Measurement and Prediction of Tip Leakage Losses in an Axial-Flow Transonic Turbine", 97-GT-203, Int. Gas Turbine Conference, Orlando, USA.

Yang, T.T. and Diller, T.E., 1995, "Heat Transfer and Flow for a Grooved Turbine Blade Tip in a Transonic Cascade", 95-WA/HT-29, Int. Mech. Engineering Congress & Expo.

Downloaded from http://asmedigitalcollection.asme.org/GT/proceedings-pdf/GT1999/78606/V003T01A049/2412453/v003t01a049-99-gt-169.pdf by guest on 21 August 2022